arXiv:0811.1230v1 [cond-mat.mes-hall] 8 Nov 2008

Non-equilibrium transport at a dissipative quantum phase transition

Chung-Hou Chung[1], Karyn Le Hur[2], Matthias Vojta[3], and Peter Wölfle[4,5]
[1] *Electrophysics Department, National Chiao-Tung University, HsinChu, Taiwan*
[2] *Department of Physics and Applied Physics, Yale University, New Haven, CT, USA*
[3] *Institut für Theoretische Physik, Universität zu Köln, 50937 Köln, Germany*
[4] *Institut für Theorie der Kondensierten Materie, Universität Karlsruhe, 76128 Karlsruhe, Germany*
[5] *INT, Forschungszentrum Karlsruhe, 76021 Karlsruhe, Germany*
(Dated: June 21, 2024)

We pioneerly investigate the non-equilibrium transport near a quantum phase transition in a generic and relatively simple case model, the dissipative resonant level model, that has many ramifications in nanosystems. We formulate a rigorous mapping and apply a controlled frequency-dependent renormalization group approach to compute the non-equilibrium current in the presence of a finite bias voltage V. For $V \to 0$, we find that the conductance has its well-known equilibrium form, while it displays a distinct non-equilibrium profile at finite voltage.

PACS numbers: 72.15.Qm,73.23.-b,03.65.Yz

In recent years, quantum phase transitions (QPTs) [1, 2] have attracted much attention at the nanoscale [3, 4, 5, 6, 7, 8]. However, little is known about the corresponding out-of-equilibrium properties [9, 10]. In fact, a finite bias voltage applied across a nanosystem is expected to smear out the equilibrium transition, but the current-induced decoherence might act quite differently as compared to thermal decoherence at finite temperature T, resulting in exotic behavior near the transition. In this Letter, we aim to answer several fundamental questions related to the non-equilibrium transport in quantum dot settings, such as what is the scaling behavior of the conductance at zero temperature and finite bias voltage near the transition.

For this purpose, we employ a typical nano-model comprising a dissipative resonant level (quantum dot). In this model, the QPT separating the conducting and insulating phase for the level is solely driven by dissipation, which can be modeled by a bosonic bath. Dissipation-driven QPTs have been addressed theoretically and experimentally in various systems, such as: Josephson junction arrays [11], superconducting thin films [12], superconducting qubit [13] and biological systems [14].

Our Hamiltonian takes the precise form:

$$H = \sum_{k,i=1,2} (\epsilon(k) - \mu_i) c^\dagger_{ki} c_{ki} + t_i c^\dagger_{ki} d + h.c. \qquad (1)$$
$$+ \sum_r \lambda_r (d^\dagger d - 1/2)(b_r + b^\dagger_r) + \sum_r \omega_r b^\dagger_r b_r,$$

where t_i is the (real) hopping amplitude between the lead i and the quantum dot, c_{ki} and d are electron operators for the (Fermi-liquid type) leads and the quantum dot, respectively. $\mu_i = \pm V/2$ is the chemical potential applied on the lead i, while the dot level is at zero chemical potential. To simplify the discussion, we assume that the electron spins have been polarized through the application of a strong magnetic field. Here, b_α are the boson operators of the dissipative bath, that is governed by the Ohmic type spectral density [4]: $J(\omega) = \sum_r \lambda_r^2 \delta(\omega - \omega_r) = \alpha\omega$,

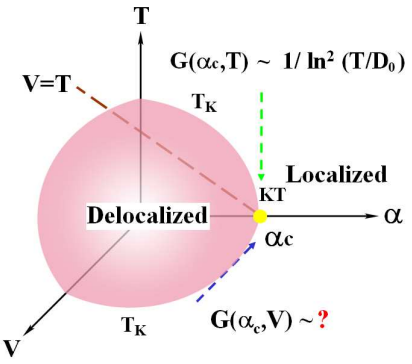

FIG. 1: Phase diagram of a resonant-level model as a function of temperature T, dissipation strength α, and bias voltage V.

and the Planck constant $\hbar$ has been set to unity.

In equilibrium ($V = 0$), such a dissipative system comprising several leads maps onto the anisotropic one-channel Kondo model; we denote by t the hopping amplitude between the (effective) lead and the level. We introduce the dimensionless transverse Kondo coupling $g^{(e)}_\perp$ which is proportional to t (the exact prefactor is given in Refs. [4, 5, 6]) as well as the longitudinal coupling $g^{(e)}_z \propto 1 - \sqrt{\alpha}$ [4, 5, 6]. The model exhibits a Kosterlitz-Thouless (KT) QPT from a delocalized (Kondo screened) phase for $g^{(e)}_\perp + g^{(e)}_z > 0$, with a large (near unitary) conductance, $G \approx e^2/h$, to a localized (local moment) phase for $g^{(e)}_\perp + g^{(e)}_z \leq 0$, with a small conductance, as the dissipation strength is increased (see Fig. 1). For $g^{(e)}_\perp \to 0$, the KT transition occurs at $\alpha_c = 1$. As $\alpha \to \alpha_c$, the Kondo temperature T_K obeys $\ln T_K \propto 1/(\alpha - \alpha_c)$ [3].

In equilibrium, the scaling functions $g^{(e)}_\perp(T)$ and $g^{(e)}_z(T)$ are obtained via the renormalization-group (RG) equations of the anisotropic Kondo model: $g^{(e)}_{\perp,cr}(T) = -g^{(e)}_{z,cr}(T) = (2\ln(\mathcal{D}/T))^{-1}$, where $\mathcal{D} = D_0 e^{1/(2g_\perp)}$, with D_0 being the ultraviolet cutoff and we set the Boltzmann constant $k_B = 1$. Having in mind a quantum dot at reso-

nance, $D_0 = \min(\delta\epsilon, \omega_c)$, with $\delta\epsilon$ being the level spacing on the dot and ω_c the cut-off of the bosonic bath; D_0 is of the order of a few Kelvins. The conductance at the quantum phase transition drops abruptly [7]:

$$G_{eq}(\alpha_c, T) \propto \left[g^{(e)}_{\perp,cr}(T)\right]^2 \propto \frac{1}{\ln^2(T/\mathcal{D})}. \qquad (2)$$

Below, we analyze the nonequilibrium ($V \neq 0$) transport at the phase transition and in the localized phase.

First, we envision a non-equilibrium mapping revealing that the leads are controlled by distinct chemical potentials. Through similar bosonization and refermionization procedures as in equilibrium [3, 4, 5, 6], our model is mapped onto an anisotropic Kondo model with the effective (Fermi-liquid) left (L) and right lead (R) [15]:

$$\begin{aligned} H_K &= \sum_{k,\gamma=L,R,\sigma=\uparrow,\downarrow} [\epsilon_k - \mu_\gamma] c^\dagger_{k\gamma\sigma} c_{k\gamma\sigma} \qquad (3) \\ &+ (J^1_\perp s^+_{LR} S^- + J^2_\perp s^+_{RL} S^- + h.c.) + \sum_{\gamma=L,R} J_z s^z_{\gamma\gamma} S^z, \end{aligned}$$

where $c^\dagger_{kL(R)\sigma}$ is the electron operator of the effective lead $L(R)$, with σ the spin quantum number, $S^+ = d^\dagger$, $S^- = d$, and $S^z = Q - 1/2$ where $Q = d^\dagger d$ describes the charge occupancy of the level. Additionally, $s^\pm_{\gamma\beta} = \sum_{\alpha,\delta,k,k'} 1/2 c^\dagger_{k\gamma\alpha} \sigma^\pm_{\alpha\delta} c_{k'\beta\delta}$ are the spin-flip operators between the effective leads γ and β, $J^{1(2)}_\perp \propto t_{1(2)}$ embody the transverse Kondo couplings, $J_z \propto 1/2(1 - 1/\sqrt{2\alpha^*})$, and $\mu_\gamma = \pm\frac{V}{2}\sqrt{1/(2\alpha^*)}$, where $1/\alpha^* = 1 + \alpha$. It should be noted that this mapping is exact near the phase transition where $\alpha \to 1$ or $\alpha^* \to 1/2$, and thus $\mu_\gamma = \pm V/2$.

Additionally, the averaged current I through the resonant level is equivalent to the averaged current in the effective Kondo problem. Indeed, from the mapping, we identify that $N_1 - N_2 = (N_L - N_R)$, where $N_i = \sum_{ki} c^\dagger_{ki} c_{ki}$ represents the charge in lead $i = 1, 2$, whereas $N_\gamma = \sum_k c^\dagger_{k\gamma\sigma} c_{k\gamma\sigma}$ represents the charge in the effective lead $\gamma = L, R$. We have checked that the averaged currents (to second order in the hopping amplitudes) within the Keldysh formalism are the same in the original and in the effective Kondo model. Thus, the current I can be computed from the two-lead anisotropic Kondo model.

The poor-man scaling equations of Anderson are generalized to nonequilibrium RG equations by including the frequency dependence of the Kondo couplings and the decoherence due to the steady-state current at finite bias voltage [16]. For the sake of clarity, we assume that the resonant level (quantum dot) is symmetrically coupled to the right and to the left lead, $t_1 = t_2$. The dimensionless Kondo couplings then have the extra symmetry (ω is the frequency): $g_{\perp(z)}(\omega) = g_{\perp(z)}(-\omega)$ where $g_{\perp(z)} = N(0) J_{\perp(z)}$ with $N(0)$ being the density of states per spin of the conduction electrons. We obtain [16]:

$$\begin{aligned} \frac{\partial g_z(\omega)}{\partial \ln D} &= -\sum_{\beta=-1,1} \left[g_\perp\left(\frac{\beta V}{2}\right)\right]^2 \Theta_{\omega+\frac{\beta V}{2}} \qquad (4) \\ \frac{\partial g_\perp(\omega)}{\partial \ln D} &= -\sum_{\beta=-1,1} g_\perp\left(\frac{\beta V}{2}\right) g_z\left(\frac{\beta V}{2}\right) \Theta_{\omega+\frac{\beta V}{2}}, \end{aligned}$$

where $\Theta_\omega = \Theta(D - |\omega + i\Gamma|)$, $D < D_0$ is the running cutoff, and Γ is the decoherence (dephasing) rate at finite bias which cuts off the RG flow [16]. The configurations of the system out of equilibrium are not true eigenstates, but acquire a finite lifetime. The spectral function of the fermion on the level is peaked at $\omega = \pm V/2$, and therefore we have $g_{\perp(z)}(\omega) \approx g_{\perp(z)}(\pm V/2)$ on the right hand side of Eq. (4). Other Kondo couplings are not generated.

In the Kondo model, Γ corresponds to the relaxation rate due to spin flip processes (which are charge flips in the original model). From Ref. [16], we identify:

$$\begin{aligned} \Gamma = \frac{\pi}{4\hbar} \sum_{\gamma,\gamma',\sigma} \int d\omega \Big[& n_\sigma g^2_z(\omega) f_{\omega-\mu_\gamma}(1 - f_{\omega-\mu_{\gamma'}}) \qquad (5) \\ & + n_\sigma g^2_\perp(\omega) f_{\omega-\mu_\gamma}(1 - f_{\omega-\mu_{\gamma'}}) \Big], \end{aligned}$$

where f_ω is the Fermi function. Here, $\gamma = \gamma'$ for the $g^2_z(\omega)$ terms while $\gamma \neq \gamma'$ for the $g^2_\perp(\omega)$ terms with γ, γ' being L or R. We have introduced the occupation numbers n_σ for up and down spins satisfying $n_\uparrow + n_\downarrow = 1$ and $S_z = 1/2(n_\uparrow - n_\downarrow)$. In the delocalized phase, we get $n_\uparrow = n_\downarrow = 1/2$ in agreement with the quantum Boltzmann equation [16]; at the phase transition we can use that $g_\perp(\omega) = -g_z(\omega)$ and that $\sum_\sigma n_\sigma = 1$, and in the localized phase $g_\perp \leq -g_z$, n_σ satisfies $|S_z| \to 1/2$ [3, 4, 5, 6].

Following the scheme of Ref. [16], we solve Eqs. (4) and (5) self-consistently. First, we compute $g_{\perp(z)}(\omega = \pm V/2)$ for a given cutoff D. Second, we substitute the solutions back into the RG equations to get the general solutions for $g_{\perp(z)}(\omega)$ at finite V, and then extract the solutions in the limit $D \to 0$. When the cutoff D is lowered, the RG flows are not cutoff by V but continue to flow for $\Gamma < D < V$ until they are stopped for $D < \Gamma$.

At the KT transition, we both numerically and analytically solve Eqs. (4) and (5) (in the limit of $D \to 0$):

$$\begin{aligned} g_{\perp,cr}(\omega) &= \sum_\beta \Theta(|\omega - \beta V/2| - V) \frac{1}{4\ln\left[\frac{\mathcal{D}}{|\omega-\beta V/2|}\right]} \qquad (6) \\ &+ \Theta(V - |\omega - \beta V/2|) \times \\ &\left[\frac{1}{\ln[\mathcal{D}^2/V \max(|\omega - \beta V/2|, \Gamma)]} - \frac{1}{4\ln\frac{\mathcal{D}}{V}}\right]. \end{aligned}$$

The solutions are shown in Fig. 2. Since $g_\perp(\omega)$ decreases under the RG scheme at the KT transition, the effect of the decoherence rate leads to minima points; here, the couplings are more severely suppressed at the resonance points $\omega = \pm\frac{V}{2}$. We check that $g_{\perp,cr}(\omega) = -g_{z,cr}(\omega)$.

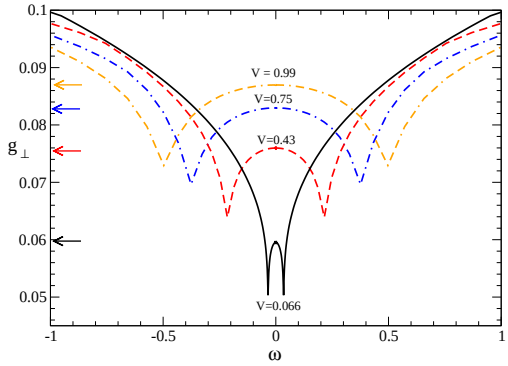

FIG. 2: $g_{\perp,cr}(\omega) = -g_{z,cr}(\omega)$ at the transition; the bare couplings are $g_\perp = -g_z = 0.1$. We have set $V = 0.066D_0$, $0.43D_0$, $0.75D_0$ and $0.99D_0$ where $D_0 = 1$ for all the figures. The arrows give the values of $g_\perp(\omega = 0)$ at these bias voltages.

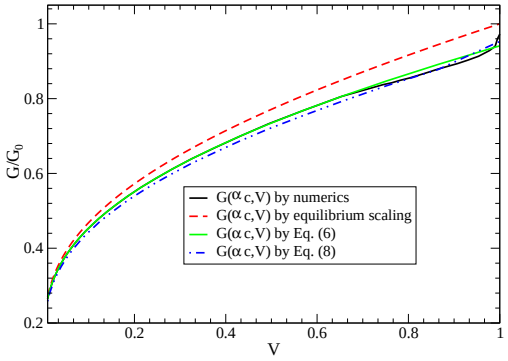

FIG. 3: Nonequilibrium conductance at the KT transition. Here, G_0 is the equilibrium conductance at the transition for $T = D_0$: $G_0 = G_{eq}(\alpha_c, T = D_0) = 0.005\pi/\hbar$ with the bare couplings $g_\perp = -g_z = 0.1$. We set the charge $e = 1$.

From the Keldysh calculation up to second order in the tunneling amplitudes, the current reads:

$$I = \frac{\pi}{8\hbar}\int d\omega\Big[\sum_\sigma 4g_\perp(\omega)^2 n_\sigma \times \qquad (7)$$
$$f_{\omega-\mu_L}(1-f_{\omega-\mu_R})\Big] - (L \leftrightarrow R).$$

At $T = 0$, it simplifies as $I = \frac{\pi}{2\hbar}\int_{-V/2}^{V/2} d\omega g_\perp^2(\omega)$. Then, we numerically evaluate the nonequilibrium current. The conductance is obtained from $G(V) = dI/dV$. The $T = 0$ results at the KT transition are shown in Fig. 3. First, it is instructive to compare the non-equilibrium current at the transition to the approximate expression:

$$I(\alpha_c, V) \approx \frac{\pi V}{2\hbar}\left(\frac{\pi}{4}\left[g_{\perp,cr}(\omega = 0)\right]^2\right) \qquad (8)$$
$$+ \frac{\pi V}{2\hbar}\left((1-\frac{\pi}{4})\left[g_{\perp,cr}(\omega = V/2)\right]^2\right),$$

where $g_{\perp,cr}(\omega = 0) \approx 2\left(\frac{1}{\ln(2\mathcal{D}^2/V^2)} - \frac{1}{4\ln(\mathcal{D}/V)}\right)$, and $g_{\perp,cr}(\omega = V/2) \approx 1/\ln(\frac{\mathcal{D}^2}{IV})$. We have treated $g_{\perp,cr}(\omega)^2$ within the interval $-V/2 < \omega < V/2$ as a semi-ellipse.

As demonstrated in Fig. 3, the conductance $G(V)$ obtained via the approximation in Eq. (8) fits very well with that obtained numerically over a whole range of $0 < V < D_0$. In the low-bias $V \to 0$ (equilibrium) limit, since $g_{\perp,cr}(\omega = 0) \approx g^{(e)}_{\perp,cr}(T = V) \ll 1$, we have $I(\alpha_c, V) \approx \frac{\pi V}{2\hbar}\left(g^{(e)}_{\perp,cr}(T = V)\right)^2$; therefore the scaling of $G(\alpha_c, V)$ is reminiscent of the equilibrium expression in Eq. (2), $G(\alpha_c, V) \approx \frac{\pi}{2\hbar}\left(g^{(e)}_{\perp,cr}(T = V)\right)^2 = \frac{\pi}{8\hbar}\frac{1}{\ln^2(\mathcal{D}/V)}$. This agreement between equilibrium and nonequilibrium conductance at low V persists up to a crossover scale $V \approx 0.01D_0$ (determined for the parameters used in Fig. 3). At larger biases, the conductance shows a unique nonequilibrium profile; see Eq. (8). We find an excellent agreement of the nonequilibrium conductance obtained by three different ways — pure numerics, analytical solution Eq. (6) and the approximation in Eq. (8).

The distinct nonequilibrium scaling behavior seen here is in fact closely tied to the non-trivial (non-linear) V dependence of the decoherence rate $\Gamma(V)$. In particular, at the KT transition, we find that $\Gamma \sim \frac{1}{2}I$ is a highly non-linear function in V, resulting in the deviation of the nonequilibrium scaling from that in equilibrium at large bias voltages. In the high bias limit ($V \to D_0$), since $g_\perp(\omega)$ approaches its bare value $g_\perp(\omega) \to g_\perp$, the nonequilibrium conductance increases more rapidly and approaches $G(\alpha_c, V) \approx G_0 = \frac{\pi}{2\hbar}g_\perp^2$. The nonequilibrium conductance is always smaller than the equilibrium one, $G(\alpha_c, V) < G_{eq}(\alpha_c, T = V)$.. This stems from the fact that the RG flows of $g_\perp(\omega = \pm V/2)$ are cutoff by the decoherence Γ, then resulting in $g_\perp(\omega = \pm V/2) < g_\perp(\omega = 0)$. Additionally, in the delocalized phase for $V \gg T_K > 0$, since the RG flow of $g_\perp$ is suppressed by the decoherence rate, we predict $G \propto 1/\ln^2(V/T_K)$ [16].

In the localized phase, the equilibrium RG equations of the effective Kondo model can be solved analytically, resulting in $G^{(e)}_{loc}(T) = \frac{\pi}{2\hbar}\left(g^{(e)}_{\perp,loc}(T)\right)^2$, where $g^{(e)}_{\perp,loc}(T) = \frac{2cg_\perp(c+|g_z|)}{(c+|g_z|)^2-g_\perp^2}(\frac{T}{D_0})^{2c}$ with $c = \sqrt{g_z^2 - g_\perp^2}$. We introduce the energy scale $T^* = D_0 e^{-\pi/\sqrt{g_z^2-g_\perp^2}}$ (which vanishes at the KT transition) such that $g^{(e)}_{\perp,loc}(T) \propto (T/T^*)^{2c}$ for $T \to 0$, leading to $G^{(e)}_{loc}(T) \propto (T/T^*)^{4c}$.

For very small bias voltages $V \to 0$, we find that the conductance reduces to the equilibrium scaling: $G(V) \to G^{(e)}_{loc}(T = V) \propto (V/T^*)^{4c}$ (see Fig. 4 (a) and Fig. 4 (b)). For $g_\perp \ll |g_z|$ and $\alpha^* \to 1/2$, we get that the exponent $4c \approx 2\alpha^* - 1$, in perfect agreement with that obtained in equilibrium at low temperatures: $G(T) \propto T^{2\alpha^*-1}$ [7]. At higher bias voltages $0.01D_0 < V < D_0$, the conductance now follows a unique nonequilibrium form (consult Fig. 4(c)) whose qualitative behavior is similar to that at the KT transition. Moreover, we have extracted rigorous so-

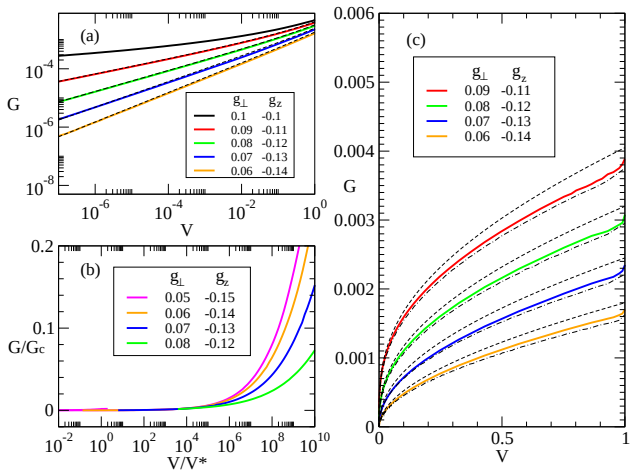

FIG. 4: Conductance in the localized phase (in units of $\pi/\hbar$). (a) $G(V)$ at low bias follows the equilibrium scaling (dashed lines). (b) The conductance $G(V)/G_c$ is a function of V/T^* where we have defined $G_c = G(\alpha_c, V)$ and $T^* = D_0 e^{-\pi/\sqrt{g_z^2 - g_\perp^2}}$. (c) At large bias voltages V, the nonequilibrium conductance $G(V)$ (solid lines) is distinct from the equilibrium form (dashed lines). The dot-dashed lines stem from an analytical approximation via Eq. (8).

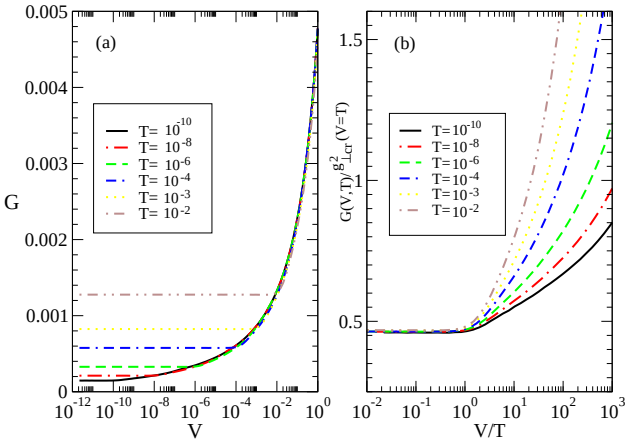

FIG. 5: V/T scaling of the conductance at the KT transition (same unit as in Fig. 3). (a). For $V > T$, the conductance follows the nonequilibrium scaling $G(\alpha_c, V)$. (b). For $V < T$, now the conductance follows the equilibrium scaling $G(\alpha_c, T)$.

lutions for $g_{\perp/z}(\omega = \pm V/2, 0)$, but the expressions are certainly too involved to be shown in this Letter.

We have also analyzed the finite temperature profile of the nonequilibrium conductance at the transition. We distinguish two different behaviors. For $V > T$, the conductance $G(V,T)$ follows the nonequilibrium form at $T = 0$ (see Fig. 5(a)), while for $V < T$ it follows the $(V = 0)$ finite-temperature expression (see Fig. 5(b)). These two scaling behaviors have a crossover at $V = T$.

In summary, we have investigated the nonequilibrium transport at a QPT using a standard nano-model, the dissipative resonant level. We have envisaged an exact mapping and applied a controlled frequency-dependent renormalization group approach to compute the current. For $V \to 0$, the conductance G follows the equilibrium behavior; by increasing V, the frequency-dependence of the couplings begin to play an important role and therefore we systematically find very distinct and precise scalings. We have also analyzed the finite temperature profile of $G(V,T)$ at the transition and identified two distinct behaviors at $V > T$ and $V < T$. Our results have a direct experimental relevance for dissipative two-level systems.

We are grateful to D. Goldhaber-Gordon and G. Zarand for stimulating discussions, and to R.T. Chang and K.V.P. Lata for technical support. We also acknowledge the generous support from the NSC grant No.95-2112-M-009-049-MY3, the MOE-ATU program, the NCTS of Taiwan, R.O.C. (C.H.C.), the Department of Energy in USA under the contract DE-FG02-08ER46541 (K.L.H.), the DFG via SFB 608 and SFB/TR-12 (M.V.), and the DFG-Center for Functional Nanostructures, C.F.N. (P.W.). C.H.C. has also benefitted from the visiting programs of KITP, ICTP, and MPI-PKS.

[1] S. Sachdev, *Quantum Phase Transitions*, Cambridge University Press (2000).
[2] S. L. Sondhi, S. M. Girvin, J. P. Carini, and D. Shahar, Rev. Mod. Phys. **69**, 315 (1987).
[3] K. Le Hur, Phys. Rev. Lett. **92**, 196804 (2004); M.-R. Li, K. Le Hur, and W. Hofstetter, Phys. Rev. Lett. **95**, 086406 (2005).
[4] K. Le Hur and M.-R. Li, Phys. Rev. B **72**, 073305 (2005).
[5] P. Cedraschi and M. Büttiker, Annals of Physics (NY) **289**, 1 (2001).
[6] A. Furusaki and K. A. Matveev, Phys. Rev. Lett. **88**, 226404 (2002).
[7] L. Borda, G. Zarand, and D. Goldhaber-Gordon, cond-mat/0602019.
[8] G. Zarand, C.-H. Chung, P. Simon, and M. Vojta, Phys. Rev. Lett. 97, 166802 (2006).
[9] A. Mitra *et al.*, Phys. Rev. Lett., **97**, 236808 (2006)
[10] R. M. Potok, I. G. Rau, H. Shtrikman, Y. Oreg, and D. Goldhaber-Gordon, Nature **447**, 167 (2007).
[11] G. Refael, E. Demler, Y. Oreg, and D. S. Fisher, Phys. Rev. B **75**, 014522 (2007).
[12] N. Mason and A. Kapitulnik, Phy. Rev. B **65**, 220505 (2002).
[13] A. J. Rimberg *et al.*, Phys. Rev. Lett. **78**, 2632 (1997).
[14] J. Gilmore and R. McKenzie, J. Phys. C. **11**, 2965 (1999).
[15] In the delocalized phase, it would be more judicious to redefine $\Psi \to (t_1 c_1 + t_2 c_2)/\sqrt{t_1^2 + t_2^2}$, and then bosonize and refermionize to get the fermions with spins [4], Ψ_σ. For $V \ll T_K$: $\Psi_\uparrow^\dagger \Psi_\downarrow \leftarrow 1/\sqrt{t_1^2 + t_2^2}(t_1 c_{L\uparrow}^\dagger c_{R\downarrow} + t_2 c_{R\uparrow}^\dagger c_{L\downarrow})$ and $\Psi_\sigma^\dagger \Psi_\sigma \leftarrow (1/\sqrt{t_1^2 + t_2^2}) \sum_{\alpha=L,R} t_\alpha c_{\alpha\sigma}^\dagger c_{\alpha\sigma}$.
[16] A. Rosch, J. Paaske, J. Kroha, and P. Wölfle, Phys. Rev. Lett. **90**, 076804 (2003); J. Phys. Soc. Jpn. **74**, 118 (2005).